CHINESE OPTICS LETTERS

Vol. 23, No. 1 | January 2025

Dispersions of two-photon and three-photon absorption in GaS films from 540 to 1600 nm

Yijie Wang (王艺洁), Jinhong Liu (刘晋红), Yanqing Ge (葛燕青), Erkang Li (李二康), Lili Zhao (赵丽丽), Chunhui Lu (卢春辉)*, Yixuan Zhou (周译玄)**, and Xinlong Xu (徐新龙)***

Shaanxi Joint Laboratory of Graphene, State Key Laboratory Incubation Base of Photoelectric Technology and Functional Materials, International Collaborative Center on Photoelectric Technology and Nano Functional Materials, Institute of Photonics & Photon-Technology, School of Physics, Northwest University, Xi'an 710069, China

*Corresponding author: luchunhui@nwu.edu.cn

**Corresponding author: yxzhou@nwu.edu.cn

***Corresponding author: xlxuphy@nwu.edu.cn

Received June 22, 2024 | Accepted July 26, 2024 | Posted Online February 4, 2025

The development of nonlinear optical materials with strong multiphoton absorption (MPA) is crucial for the design of ultrafast nonlinear optical devices, such as optical limiters and all-optical switchers. In this study, we present the wavelength-dependent coefficients of two-photon absorption (2PA) and three-photon absorption (3PA) in a GaS film across a broad range of wavelengths from 540 to 1600 nm. The observed dispersions in the 2PA and 3PA coefficients align well with the widely used two-band approximation model applied to direct bandgap semiconductors. Notably, the GaS film exhibits exceptional MPA properties with a maximum 2PA coefficient of 19.89 cm/GW at 620 nm and a maximum 3PA coefficient of 4.88 cm^3/GW^2 at 1500 nm. The GaS film surpasses those found in traditional wide-bandgap semiconductors like β-Ga_2O_3, GaN, ZnO, and ZnS while remaining comparable to monolayer MoS_2, $CsPbBr_3$, and $(C_4H_9NH_3)_2PbBr_4$ perovskites. By employing a simplified two-energy-level model analysis, our results indicate that these large MPA coefficients are primarily determined by the remarkable absorption cross sections, which are approximately 4.82×10^{-52}·cm^4·s·$photon^{-1}$ at 620 nm for 2PA and 8.17×10^{-80}·cm^6·s^2·$photon^{-2}$ at 1500 nm for 3PA. Our findings demonstrate significant potential for utilizing GaS films in nonlinear optical applications.

Keywords: GaS film; multiphoton absorption; two-photon absorption; three-photon absorption; dispersion.
DOI: 10.3788/COL202523.011901

1. Introduction

Multiphoton absorption (MPA) has garnered significant attention in the fields of optical power limiting and ultrafast all-optical switching applications due to its effective control and modulation of optical signals[1,2]. Nonlinear optical (NLO) materials play a crucial role in realizing such photonic devices, necessitating high optical nonlinearity, low linear optical losses, and ultrafast response time[3]. In this regard, wide-gap semiconductors have emerged as promising candidates for these requirements owing to their weak absorption from one-photon transitions and large nonlinearity at communication wavelengths. Recent investigations have extensively explored the two-photon absorption (2PA) and three-photon absorption (3PA) properties of β-Ga_2O_3[4], ZnO[5], ZnS[6], and GaN[7] through experimental measurements and theoretical calculations. However, these bulk semiconductors exhibit relatively low nonlinear coefficients (2PA coefficient $\beta_2 \sim 10$ cm/GW and 3PA coefficient $\beta_3 \sim 10^{-3}$–10^{-4} cm^3/GW^2), relatively slow relaxation time (tens to hundreds of picoseconds), as well as substantial lattice mismatch that hinder their application in integrated photonic platforms. The utilization of 2D materials offers new opportunities for the development of ultrafast and miniaturized photonic devices due to their significant third-order and high-order NLO absorption, ease of integration, and small lattice mismatch[8].

A recent study has demonstrated that 2D GaP achieves ultrafast sub-30 fs all-optical switching based on the optical Kerr effect and 2PA[1]. Similarly, hexagonal phase GaS also exhibits high stability, tunable bandgap (2.3–3.2 eV), and strong optical absorption[9]. In the field of NLO, recent advancements in nanoscale GaS have shown excellent saturable absorption (SA) properties and successful applications in ultrafast mode-locking[10]. Additionally, odd-layer GaS possesses a noncentrosymmetric nature with a strong second-order susceptibility of approximately 47.98 pm/V[11]. In terms of MPA property research, previous experimental investigations on the 2PA of the GaS thin film at a single wavelength of 650 nm reveal that the 2PA

coefficient is in the order of 10^3 scale, much higher than conventional wide-bandgap semiconductors[12], making GaS a promising candidate for designing high-performance all-optical switches and optical limiters. Therefore, direct measurement and systematic analysis of the dispersion characteristics of both 2PA and 3PA spectra in the GaS thin film are crucial for promoting relevant application development.

In this Letter, we present a comprehensive investigation of the 2PA and 3PA spectra of GaS thin film in the spectral range of 540–1600 nm using a femtosecond Z-scan system. Both the 2PA and 3PA spectra exhibit excellent agreement with theoretical analysis based on the two-band approximation model for direct bandgap semiconductors. The measured maximum values are approximately 19.89 cm/GW at 620 nm for β_2 and approximately 4.88 cm^3/GW^2 at 1500 nm for β_3, which significantly surpass those reported for previously studied wide-bandgap semiconductors. Based on a simplified two-energy level model, our findings reveal that the GaS film not only exhibits a large cross section of 2PA (4.82×10^{-52} $cm^4 \cdot s \cdot photon^{-1}$ at 620 nm) but also demonstrates a strong cross section of 3PA (8.17×10^{-80} $cm^6 \cdot s^2 \cdot photon^{-2}$ at 1500 nm). These results underscore the immense potential of wide-bandgap 2D materials possessing exceptional MPA for applications in NLO.

2. Results and Discussion

The GaS thin film was synthesized using a physical vapor deposition (PVD) technique. In the experimental setup, 20 mg of GaS powder was placed at the center of a tube furnace with a heating zone set at 940°C to facilitate source evaporation. Subsequently, the resulting GaS vapor was transported onto a sapphire substrate using high-purity argon gas with a flow rate of 40 sccm, leading to the formation of a continuous thin film that is approximately 650 nm thick. This morphology is confirmed by a scanning electron microscope (SEM), as shown in Fig. 1(a). Additionally, the micro-Raman spectrum shown in Fig. 1(b) exhibits three characteristic peaks at 182.8, 286.4, and 357.1 cm^{-1} corresponding to the A^1_{1g}, E^1_{2g}, and A^2_{1g} phonon modes respectively, thereby indicating successful preparation of the GaS film. Furthermore, X-ray diffraction (XRD) spectroscopy confirms the absence of byproducts such as Ga_2S_3 during synthesis. This is evident from Fig. 1(c), which exhibits three prominent peaks at 11.60°, 23.07°, and 34.81° corresponding to the (002), (004), and (006) planes for hexagonal GaS (PDF#08-0417). Moreover, the peaks at 30.72° and 35.53° originate from the substrate. The narrow half-widths observed indicate a high degree of crystallinity and purity in our samples. Further characterization through UV-Vis absorption measurements reveals significant optical absorption within the wavelength range of 400 to 500 nm [Fig. 1(d)]. Based on Tauc plot analysis, the intrinsic bandgap energy of GaS is estimated to be approximately 2.3 eV, consistent with previous reports[11].

The dispersion of the nonlinear coefficient (β) in the GaS film was investigated using a broadband Z-scan system. In this study, we utilized an optical parametric amplifier (TOPAS-Prime)

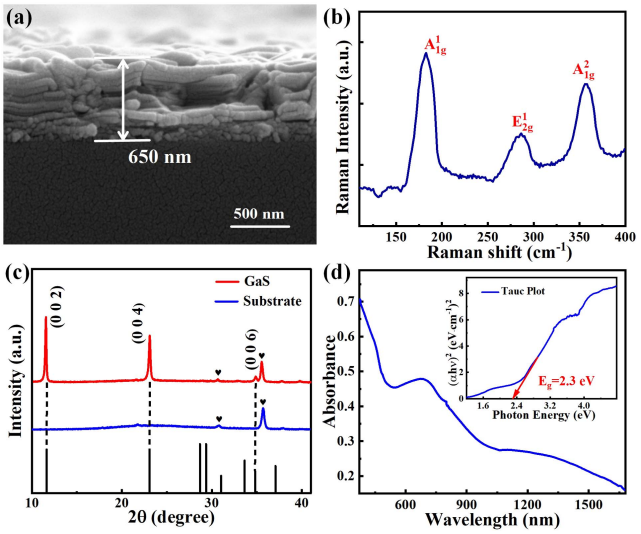

Fig. 1. (a) SEM image, (b) Raman spectrum with an excitation wavelength of 532 nm, (c) XRD pattern, and (d) linear absorption spectrum and Tauc plot of the synthesized GaS film.

pumped by a Ti:sapphire femtosecond laser operating at a center wavelength of 800 nm with a repetition rate of 1 kHz as the laser source. The output laser from the optical parametric amplifier covered a wavelength range spanning from 540 to 1600 nm. Figure 2(a) depicts the open aperture Z-scan curves obtained under excitation wavelengths ranging from 540 to 1040 nm. The decrease in normalized transmittance as the sample approaches the focal point ($Z = 0$) clearly indicates a reverse saturable absorption (RSA) response, which can be attributed to phenomena such as nonlinear scattering, excited state absorption (ESA), and MPA[13]. Considering our GaS film's uniform thickness without any scattering centers, we can neglect the contribution of nonlinear scattering, which is further confirmed by relocating the photodetector position and observing no

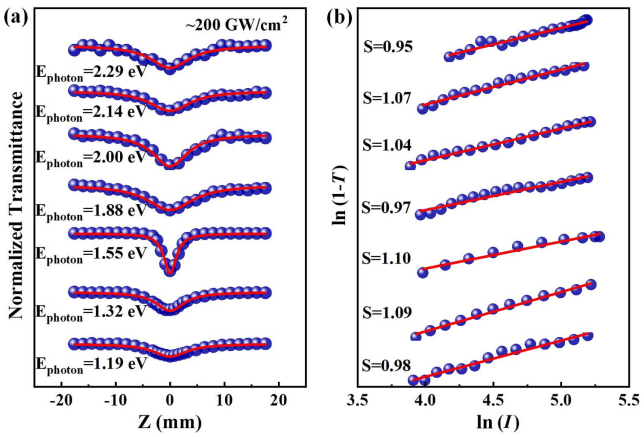

Fig. 2. (a) Open aperture Z-scan traces of the GaS film with excitation wavelengths of 540, 580, 620, 660, 800, 940, and 1040 nm at a pump intensity of about 200 GW/cm^2. (b) The plots of ln (1−T) versus ln (I) to validate the order of nonlinearity, with solid lines representing the theoretical fitting.

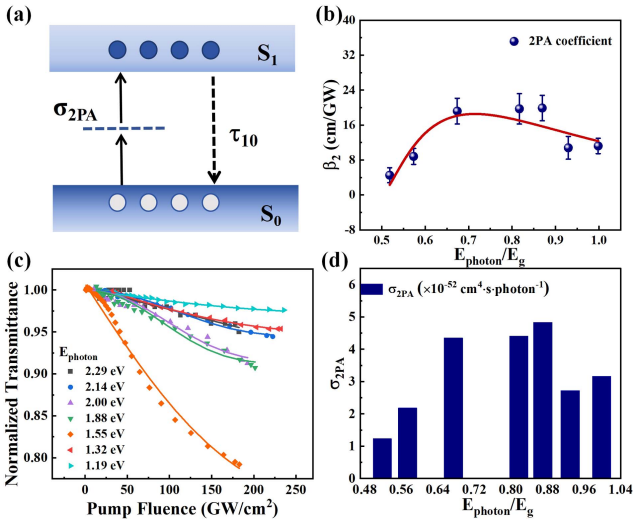

Fig. 3. (a) Two-level system used to model the 2PA process. (b) Dispersion of 2PA coefficients as a function of E_{photon}/E_g for GaS films, with solid lines representing theoretical fitting. (c) Normalized transmittance as a function of laser intensity under excitation wavelengths ranging from 540 to 1040 nm. (d) The fitted σ_{2PA} parameters based on the two-level system.

scattering signal[14]. According to the estimated bandgap above the excitation photon energy, the phenomenon of ESA is eliminated, and MPA becomes the dominant effect for RSA. The NLO response of the GaS film was further characterized by fitting $\ln(1-T)$ versus $\ln(I)$ plots using linear regression analysis. As shown in Fig. 2(b), the fitted slop values closely approximate 1, with values of 0.95, 1.07, 1.04, 0.97, 1.10, 1.09, and 0.98, indicating degenerate 2PA[15]. Additionally, when excited within a photon energy range between E_g and $1/2E_g$ via wavelengths spanning from 540 to 1040 nm, it supports a 2PA transition process. Considering that the femtosecond pulse width is shorter than the excited state lifetime, we propose a two-energy-level model to elucidate the optical absorption process as illustrated in Fig. 3(a)[16], where under laser excitation most electrons in the first excited state (S_1) rapidly return back into the ground state (S_0) while higher excited state absorptions can be ignored.

Based on the aforementioned analysis, we can quantitatively analyze the β_2 variation by employing Eq. (1) as follows[17,18]:

$$T_{\mathrm{MPA}}(z) = 1 - \frac{1}{M^{3/2}} \frac{\beta_M I_0^{M-1} L_{\mathrm{eff}}^{(M)}}{(1 + z^2/z_0^2)^{M-1}}, \tag{1}$$

where z_0 represents the Rayleigh length of the laser beam, I_0 denotes the incident intensity at focus, L_{eff} is the effective thickness of the GaS film, and M corresponds to M photon absorption.

The fitting results, represented by the solid lines in Fig. 3(b), exhibit excellent agreement with the experimental data points. The β_2 values of the GaS film are 11.21 ± 1.76 cm/GW (540 nm @ 2.29 eV), 10.79 ± 2.59 cm/GW (580 nm @ 2.14 eV), 19.89 ± 2.92 cm/GW (620 nm @ 2.00 eV), 19.71 ± 3.48 cm/GW (660 nm @ 1.88 eV), 19.19 ± 2.95 cm/GW (800 nm @ 1.55 eV), 8.82 ± 1.82 cm/GW (940 nm @ 1.32 eV), and 4.51 ± 1.71 cm/GW (1040 nm @ 1.19 eV). The results demonstrate that the β_2 values reach their maximum at 0.7 E_{photon}/E_g and subsequently exhibit a declining trend with increasing E_{photon}/E_g. More importantly, the β_2 values of the GaS film are considerably larger compared to wide bandgap semiconductors, such as β-Ga_2O_3[4,19], GaN[7], and ZnO[5] listed in Table 1. This can be attributed to the quantum confinement in 2D materials and strong light–matter interaction[20,21]. It is worth noting that the β_2 value of GaS is lower compared to previously reported β-GaS film, which can be attributed to the much higher intensity of our excitation laser. The evidently remarkable potential of the GaS film for NLO devices within the visible spectral region is apparent. Furthermore, the dispersion behavior observed in the GaS film aligns well with theoretical predictions based on Wherrett's two-band and perturbation theory[22,23], in which the 2PA dispersion relation can be described by

$$\beta_2 = 2^9 \sqrt{2}\pi \left(\frac{e^2}{\hbar c}\right)^2 \frac{f_2}{f} \frac{\hbar P}{n^2 E_g^3} \frac{(2\hbar\omega/E_g - 1)^{3/2}}{(2\hbar\omega/E_g)^5}, \tag{2}$$

where c represents the speed of light, E_g denotes the material's bandgap, n signifies its refractive index, P corresponds to the Kane momentum parameter[7], f_2 accounts for numerical factors, and $\hbar\omega$ is the photon energy.

According to the simplified two-level system, rate equations and nonlinear propagation equations can be expressed as

Table 1. The Summary of 2PA and 3PA Coefficients as Reported in the Literature.

Material	Laser source	β_2 (cm/GW)	β_3 (cm^3/GW^2)	Ref.
β-Ga_2O_3	350 nm, 190 fs	1.8	—	[19]
	570 nm, 190 fs	—	3.7×10^{-4}	[4]
	750 nm, 190 fs	—	0.8×10^{-4}	
β-GaS	650 nm, 190 fs	4900	—	[12]
GaN	500 nm, 190 fs	6.2	—	[7]
	532 nm, 18 fs	8.5	—	
	860 nm, 190 fs	—	1.8×10^{-3}	
	1000 nm, 190 fs	—	3.5×10^{-3}	
ZnO	650 nm, 150 fs	~1	—	[5]
	860 nm, 150 fs	—	$\sim 2 \times 10^{-3}$	
ZnS	780 nm, 120 fs	—	0.024	[6]
MoS_2	1300 nm, 150 fs	—	2.2	[24]
$(C_4H_9NH_3)_2PbBr_4$	1030 nm, 110 fs	—	~2	[25]
GaS	620 nm, 60 fs	19.89	—	this work
	1500 nm, 52 fs	—	4.88	

$$\frac{\partial N_0}{\partial t} = -\sigma_{2\mathrm{PA}} N_0 \frac{I^2}{2\hbar\omega} + \frac{N_1}{\tau_{10}}, \tag{3}$$

$$\frac{\partial N_1}{\partial t} = \sigma_{2\mathrm{PA}} N_0 \frac{I^2}{2\hbar\omega} - \frac{N_1}{\tau_{10}}, \tag{4}$$

$$N = N_0 + N_1. \tag{5}$$

The propagation equation in the sample is described as

$$\frac{\mathrm{d}I}{\mathrm{d}z} = -\alpha(I) = -\alpha_0 - \alpha_{\mathrm{NL}}, \tag{6}$$

where $\alpha_{\mathrm{NL}} = \sigma_{2\mathrm{PA}} N_0 I^2$. By employing the Runge–Kutta method to fit the experimental data in Fig. 3(c) with Eqs. (3)–(6), it is possible to extract the 2PA cross section ($\sigma_{2\mathrm{PA}}$) and relaxation time (τ_{10}). The τ_{10} of GaS has been measured approximately at (85 ± 19) ps[12], which serves as the fitting range. Based on this, the fitted $\sigma_{2\mathrm{PA}}$ values of GaS are determined as follows: 3.16×10^{-52} cm^4 · s · photon^{-1} (540 nm), 2.72×10^{-52} cm^4 · s · photon^{-1} (580 nm), 4.83×10^{-52} cm^4 · s · photon^{-1} (620 nm), 4.40×10^{-52} cm^4 · s · photon^{-1} (660 nm), 4.35×10^{-52} cm^4 · s · photon^{-1} (800 nm), 2.18×10^{-52} cm^4 · s · photon^{-1} (940 nm), and 1.23×10^{-52} cm^4 · s · photon^{-1} (1040 nm). The results further demonstrate that the wavelength-dependent 2PA cross section is consistent with the 2PA coefficient. Moreover, owing to its strong 2PA coefficient and ultrafast carrier lifetime characteristics, the GaS film exhibits great potential for integrated optical limiter devices.

To further investigate the dispersion characteristics of 3PA, we conducted open-aperture Z-scan measurements by increasing the excitation wavelength from 1200 to 1600 nm. As shown in Fig. 4(a), a similar RSA phenomenon is observed. Initially, we assume that the RSA induced by 3PA occurs when the incident photon energy is above $1/3E_g$ but less than $1/2E_g$. Furthermore, Fig. 4(b) demonstrates a well-fitted linear relationship between $\ln(1-T)$ and $\ln(I)$. The slopes obtained under different excitation wavelengths are close to 2, indicating degenerate 3PA for the GaS film. Under laser excitation, 3PA involves the simultaneous absorption of three photons, which leads to a transition from the ground state level (S_0) to the excited state level (S_1), as illustrated in Fig. 5(a).

Based on Eq. (1), the β_3 values of the GaS film are calculated and summarized in Fig. 5(b). The values are as follows: (1.85 ± 0.44) cm^3/GW^2 (1200 nm @ 1.03 eV), (3.35 ± 0.58) cm^3/GW^2 (1300 nm @ 0.95 eV), (5.88 ± 0.40) cm^3/GW^2 (1500 nm @ 0.83 eV), and (4.46 ± 0.59) cm^3/GW^2 (1600 nm @ 0.78 eV). The β_3 of the GaS film is larger than those of β-Ga_2O_3, GaS, GaN, ZnO, and ZnS and is comparable with monolayer MoS_2, $CsPbBr_3$, and $(C_4H_9NH_3)_2PbBr_4$ perovskites in Table 1 due to its 2D quantum confinement. Furthermore, the dependence of β_3 on E_{photon}/E_g can be well fitted by Wherrett's two-band perturbation theory equation as follows[22]:

$$\beta_3 = \frac{3^{10}\sqrt{2}}{8}\pi^2\left(\frac{e^2}{\hbar c}\right)^3 \frac{\hbar^2 P^3}{n^3 E_g^7} \frac{(3\hbar\omega/E_g - 1)^{1/2}}{(3\hbar\omega/E_g)^9}. \tag{7}$$

To gain a deeper understanding of the 3PA mechanism, a two-energy-level model is also proposed. In this scenario, the rate equation model can be given as

$$\frac{\partial N_0}{\partial t} = -\sigma_{3\mathrm{PA}} N_0 \frac{I^3}{3\hbar\omega} + \frac{N_1}{\tau_{10}}, \tag{8}$$

$$\frac{\partial N_1}{\partial t} = \sigma_{3\mathrm{PA}} N_0 \frac{I^3}{3\hbar\omega} - \frac{N_1}{\tau_{10}}, \tag{9}$$

$$N = N_0 + N_1, \tag{10}$$

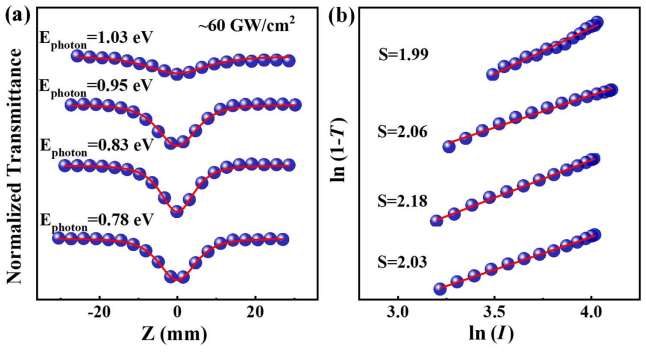

Fig. 4. (a) Open aperture Z-scan traces of the GaS film under the excitation wavelengths from 1200 to 1600 nm at the pump intensity of about 60 GW/cm^2. (b) The ln (1−T) as a function of ln(I). The solid lines represent the theoretical fitting.

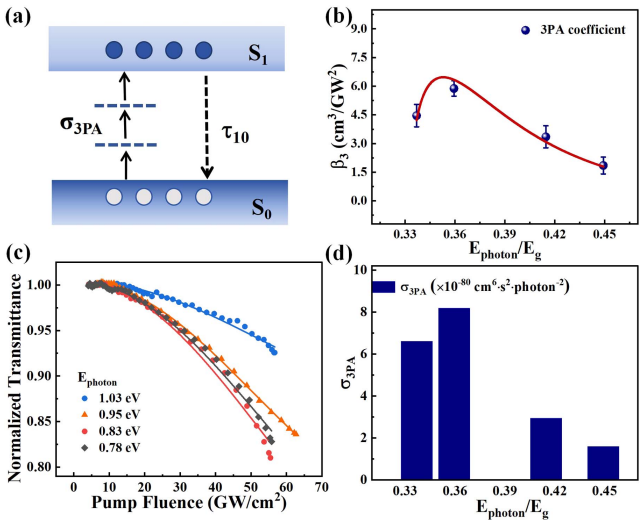

Fig. 5. (a) Two-level system used for fitting the 3PA process. (b) Dispersion of 3PA coefficients as a function of E_{photon}/E_g for GaS films, with solid lines representing theoretical fitting. (c) Normalized transmittance as a function of laser intensity under excitation wavelengths ranging from 1200 to 1600 nm. (d) The fitted $\sigma_{3\mathrm{PA}}$ parameters based on the two-level system.

$$\frac{\mathrm{d}I}{\mathrm{d}z} = -\sigma_{3\mathrm{PA}} N_0 I^3. \tag{11}$$

Here, $\sigma_{3\mathrm{PA}}$ represents the 3PA cross-section. By fitting the Z-scan experimental data in Fig. 5(c) with Eqs. (8)–(11), we obtain $\sigma_{3\mathrm{PA}}$ values of 1.59×10^{-80} cm$^6 \cdot$ s$^2 \cdot$ photon^{-2} (1200 nm), 2.93×10^{-80} cm$^6 \cdot$ s$^2 \cdot$ photon^{-2} (1300 nm), 8.17×10^{-80} cm$^6 \cdot$ s$^2 \cdot$ photon^{-2} (1500 nm), and 6.59×10^{-80} cm$^6 \cdot$ s$^2 \cdot$ photon^{-2} (1600 nm). These results further demonstrate that the larger $\sigma_{3\mathrm{PA}}$ values are responsible for the strong 3PA coefficient exhibited by the GaS film. Based on these findings, it can be concluded that the GaS film possesses significant 2PA and 3PA properties, making it a promising candidate for applications such as optical power limiting and ultrafast all-optical switching.

3. Conclusion

We conduct a systematic investigation of the dispersions of 2PA and 3PA coefficients in the GaS film using a Z-scan system equipped with a laser source ranging from 540 to 1600 nm. The observed decrease in both β_2 and β_3 values of the GaS film with increasing E_{photon}/E_g is consistent with the predictions of the two-band perturbation theory. Based on a two-energy-level model, our results reveal that the 2PA and 3PA coefficients are strongly influenced by absorption cross sections, reaching maximum values of 4.47×10^{-52} cm$^4 \cdot$ s $\cdot$ photon^{-1} at 620 nm and on the scale of 10^{-80} cm$^6 \cdot$ s$^2 \cdot$ photon^{-2} at 1500 nm, respectively. These findings demonstrate that GaS films exhibit strong MPA properties and ultrafast carrier relaxation, making them promising candidates for optical power limiting and integrated all-optical switching devices.

Acknowledgements

This work was supported by the National Natural Science Foundation of China (Nos. 12261141662 and 12074311) and the 2023 Graduate Education Comprehensive Reform Research and Practice Project (No. ZG2023009).

References

1. G. Grinblat, M. P. Nielsen, P. Dichtl, *et al.*, "Ultrafast sub–30-fs all-optical switching based on gallium phosphide," Sci. Adv. **5**, eaaw3262 (2019).
2. J. W. Perry, K. Mansour, I. Y. Lee, *et al.*, "Organic optical limiter with a strong nonlinear absorptive response," Science **273**, 1533 (1996).
3. A. Miller, K. R. Welford, and B. Daino, *Nonlinear Optical Materials and Devices for Applications in Information Technology*, Vol. **289** (Springer Science & Business Media, 2013).
4. Y. Sun, Z.-G. Li, Y. Fang, *et al.*, "Three-photon absorption and Kerr nonlinearity in pristine and doped β-Ga_2O_3 single crystals," Appl. Phys. Lett. **120**, 032101 (2022).
5. M. G. Vivas, T. Shih, T. Voss, *et al.*, "Nonlinear spectra of ZnO: reverse saturable, two-and three-photon absorption," Opt. Express **18**, 9628 (2010).
6. J. He, W. Ji, J. Mi, *et al.*, "Three-photon absorption in water-soluble ZnS nanocrystals," Appl. Phys. Lett. **88**, 181114 (2006).
7. F. Shi, Z. Li, X. Wu, *et al.*, "Broadband optical nonlinearity and all-optical switching features in low-defect GaN," Opt. Express **31**, 32263 (2023).
8. B. Guo, Q. L. Xiao, S. H. Wang, *et al.*, "2D layered materials: synthesis, nonlinear optical properties, and device applications," Laser Photonics Rev. **13**, 1800327 (2019).
9. Y. Gutiérrez, D. Juan, S. Dicorato, *et al.*, "Layered gallium sulfide optical properties from monolayer to CVD crystalline thin films," Opt. Express **30**, 27609 (2022).
10. S. Ahmed, J. Qiao, P. K. Cheng, *et al.*, "Two-dimensional gallium sulfide as a novel saturable absorber for broadband ultrafast photonics applications," ACS Appl. Mater. Interfaces **13**, 61518 (2021).
11. S. Ahmed, P. K. Cheng, J. Qiao, *et al.*, "Nonlinear optical activities in two-dimensional gallium sulfide: a comprehensive study," ACS Nano **16**, 12390 (2022).
12. H. Lu, Y. Chen, K. Yang, *et al.*, "Ultrafast nonlinear optical response and carrier dynamics in layered gallium sulfide (GaS) single-crystalline thin films," Front. Mater. **8**, 775048 (2021).
13. J. W. You, S. R. Bongu, Q. Bao, *et al.*, "Nonlinear optical properties and applications of 2D materials: theoretical and experimental aspects," Nanophotonics **8**, 63 (2018).
14. J. Huang, N. Dong, S. Zhang, *et al.*, "Nonlinear absorption induced transparency and optical limiting of black phosphorus nanosheets," ACS Photonics **4**, 3063 (2017).
15. L. Wang, S. Zhang, N. McEvoy, *et al.*, "Nonlinear optical signatures of the transition from semiconductor to semimetal in $PtSe_2$," Laser Photonics Rev. **13**, 1900052 (2019).
16. S. R. Allam and A. Sharan, "One, two and three photon absorption of two level system in femto-second laser excitation," J. Opt. **46**, 486 (2017).
17. D. S. Corrêa, L. De Boni, L. Misoguti, *et al.*, "Z-scan theoretical analysis for three-, four-and five-photon absorption," Opt. Commun. **277**, 440 (2007).
18. M. Hari, S. Mathew, B. Nithyaja, *et al.*, "Saturable and reverse saturable absorption in aqueous silver nanoparticles at off-resonant wavelength," Opt. Quantum Electron. **43**, 49 (2012).
19. X. Tian, H.-S. Lu, T. Qian, *et al.*, "Dispersion of two-photon absorption and nonlinear refraction in β-Ga_2O_3 from 350 to 515 nm," Appl. Phys. Lett. **124**, 152112 (2024).
20. X. Liu, Q. Guo, and J. Qiu, "Emerging low-dimensional materials for nonlinear optics and ultrafast photonics," Adv. Mater. **29**, 1605886 (2017).
21. C. Lu, M. Luo, Y. Ge, *et al.*, "Layer-dependent nonlinear optical properties of WS_2, MoS_2, and Bi_2S_3 films synthesized by chemical vapor deposition," ACS Appl. Mater. Interfaces **14**, 2390 (2021).
22. B. S. Wherrett, "Scaling rules for multiphoton interband absorption in semiconductors," J. Opt. Soc. Am. B **1**, 67 (1984).
23. M. Sheik-Bahae, D. C. Hutchings, D. J. Hagan, *et al.*, "Dispersion of bound electron nonlinear refraction in solids," IEEE J. Quantum Electron. **27**, 1296 (1991).
24. F. Zhou and W. Ji, "Giant three-photon absorption in monolayer mos_2 and its application in near-infrared photodetection," Laser Photonics Rev. **11**, 1700021 (2017).
25. S. Lu, F. Zhou, Q. Zhang, *et al.*, "Layered hybrid perovskites for highly efficient three-photon absorbers: theory and experimental observation," Adv. Sci. **6**, 1801626 (2019).